LETTERS

The nonlinear Fano effect

M. Kroner[1]*, A. O. Govorov[2]*, S. Remi[1], B. Biedermann[1], S. Seidl[1], A. Badolato[3], P. M. Petroff[3], W. Zhang[2], R. Barbour[4], B. D. Gerardot[4], R. J. Warburton[4] & K. Karrai[1]

The Fano effect[1] is ubiquitous in the spectroscopy of, for instance, atoms[1,2], bulk solids[3,4] and semiconductor heterostructures[5–7]. It arises when quantum interference takes place between two competing optical pathways, one connecting the energy ground state and an excited discrete state, the other connecting the ground state with a continuum of energy states. The nature of the interference changes rapidly as a function of energy, giving rise to characteristically asymmetric lineshapes. The Fano effect is particularly important in the interpretation of electronic transport[5,6] and optical spectra[7,8] in semiconductors. Whereas Fano's original theory[1] applies to the linear regime at low power, at higher power a laser field strongly admixes the states and the physics becomes rich, leading, for example, to a remarkable interplay of coherent nonlinear transitions[9]. Despite the general importance of Fano physics, this nonlinear regime has received very little attention experimentally, presumably because the classic autoionization processes[2], the original test-bed of Fano's ideas[1], occur in an inconvenient spectral region, the deep ultraviolet. Here we report experiments that access the nonlinear Fano regime by using semiconductor quantum dots, which allow both the continuum states to be engineered and the energies to be rescaled to the near infrared. We measure the absorption cross-section of a single quantum dot and discover clear Fano resonances that we can tune with the device design or even *in situ* with a voltage bias. In parallel, we develop a nonlinear theory applicable to solid-state systems with fast relaxation of carriers. In the nonlinear regime, the visibility of the Fano quantum interferences increases dramatically, affording a sensitive probe of continuum coupling. This could be a unique method to detect weak couplings of a two-level quantum system (qubits), which should ideally be decoupled from all other states.

We performed our experiments on self-assembled quantum dots. They are known to possess localized discrete energy levels, much like atoms, identified by extremely sharp lines in their optical spectra[10]. Furthermore, when the fundamental cross-gap transition is driven by a strong laser field, the electronic and photon states hybridize. Unmistakable signatures for such dressed states are Rabi oscillations[11,12], an a.c. Stark effect[10,13], and a splitting in a resonant high-Q cavity[14–17]. We use InGaAs quantum dots embedded in a GaAs vertical field-effect device[18]. The structure allows us to control the charge stored on an individual quantum dot[18] and to modulate the transition energies by applying a bias voltage, enabling high noise rejection in single dot laser spectroscopy based on modulation techniques[10].

We present here results for the X^{1-} exciton transition, which is the transition from a ground state containing a single electron to an excited state containing two electrons and a hole. Sample 1 contains a layer of InGaAs dots separated by a 25 nm tunnel barrier from a GaAs electron reservoir and by a 10 nm capping layer from an AlAs/GaAs superlattice blocking barrier (Fig. 1b). Laser spectroscopy on dots from this sample shows lorentzian lineshapes (Fig. 2a, b). At low powers, the spectra are independent of power, corresponding to behaviour in the linear regime. At powers above about ~1 nW, the spectra depend on power: this is the nonlinear regime. As the power increases, the resonance broadens and the contrast decreases, that is, the resonance saturates, exhibiting power broadening and power-induced transparency[19,20]. The behaviour follows exactly that expected for dressed states in a two-level atom. In sample 2 (Fig. 1c),

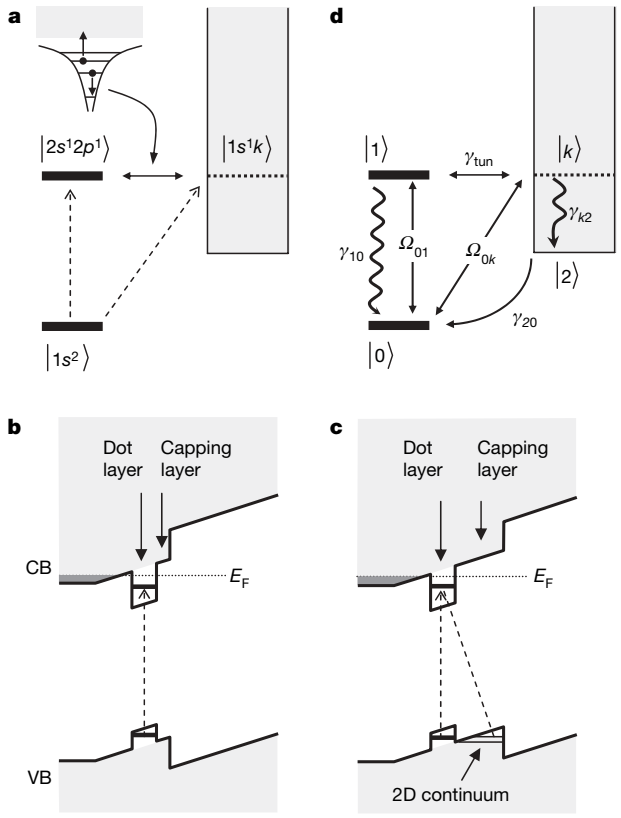

Figure 1 | Schematic level diagrams. a, Classical model of autoionization of a He atom leading to a Fano resonance in absorption. **b**, Level diagram of sample 1, showing the cross-gap exciton transition. **c**, Level diagram of sample 2. In this case, the increased capping layer thickness leads to the appearance of 2D continuum states at the interface between the capping layer and the blocking barrier. These valence continuum states couple via tunnelling with the valence dot level. **d**, Levels, transitions and relaxation processes in the model calculations. CB, conduction band; VB, valence band; E_F, Fermi energy; see text for definitions of other symbols.

[1]Center for NanoScience and Department für Physik, Ludwig-Maximilians-Universität, 80539 München, Germany. [2]Department of Physics and Astronomy, Ohio University, Athens, Ohio 45701, USA. [3]Materials Department, University of California, Santa Barbara, California 93106, USA. [4]School of Engineering and Physical Sciences, Heriot-Watt University, Edinburgh EH14 4AS, UK.
*These authors contributed equally to this work.

the thickness of the capping layer is increased from 10 nm to 30 nm but otherwise the sample was identical to the control, sample 1. In this case, we find that the behaviour at medium and high powers is markedly different: the differential absorption has undershoots and zero crossings (Fig. 2c–h), signatures of Fano-like quantum interferences.

Our key result is that the Fano effects become more and more pronounced as the laser power increases, starting out very small at low power in the linear regime but becoming unmistakable at high power in the nonlinear regime (Fig. 2). The increased visibility of the Fano interference at high laser power results from a different response of the two optical pathways. The optical transition between the discrete levels saturates at high power, but in contrast the weaker continuum transition does not saturate in the range of power we are working in. Increasing the laser power eventually enhances the continuum transition rate to match the saturated discrete level transition. Consequently, the laser power is a convenient experimental control parameter to tune the relative strength of the two competing pathways at the heart of the Fano effect.

This observation, which we back up with the theoretical consideration to follow, represents a highly sensitive technique to detect a very weak coupling between a two-level system and a continuum of extended states when the radiative lifetime of the exciton (τ_{rad}) is much less than the time required to interact with the continuum (for example, tunnelling or decay time). In the linear regime, the optical detection of very weak dot–continuum interactions is impossible because the energy uncertainty for the exciton, ΔE, obeys the Heisenberg principle $\Delta E\tau_{rad} \approx \hbar$. ΔE is equivalently the broadening of the exciton line. In other words, a strong broadening ($\Delta E \approx \hbar/\tau_{rad}$) makes the dot–continuum interaction invisible in the absorption spectrum. But in the nonlinear regime, the radiative broadening does not play the leading role, and even a very weak dot–continuum interaction becomes apparent (as shown in Fig. 2).

To verify the asymmetries shown in Fig. 2c–h as Fano interferences, we present in Fig. 3b the voltage dependence, monitoring the strength of the interference with the asymmetry parameter $1/q$, where q is the Fano factor determined at constant power. In its standard definition, q is infinite when the continuum transition is very weak, in which case the line shape is symmetric and entirely determined by the discrete transition. In contrast, when q is near unity, both the continuum and discrete optical transitions are of similar strengths, and the line shape becomes very asymmetric. The $1/q$ parameter has a strong bias dependence, disappearing towards the right-hand edge of the X^{1-} plateau. The bias dependence cannot be explained by a purely optical interference[21,22], as in this case the bias would have no effect. Instead, a Fano interference provides a natural explanation.

Optical excitation drives the system from its discrete initial state, a quantum dot containing a single electron, $|0\rangle$, to the X^{1-} state containing two electrons and one hole, $|1\rangle$ (Fig. 1d). State $|1\rangle$ is in tunnel

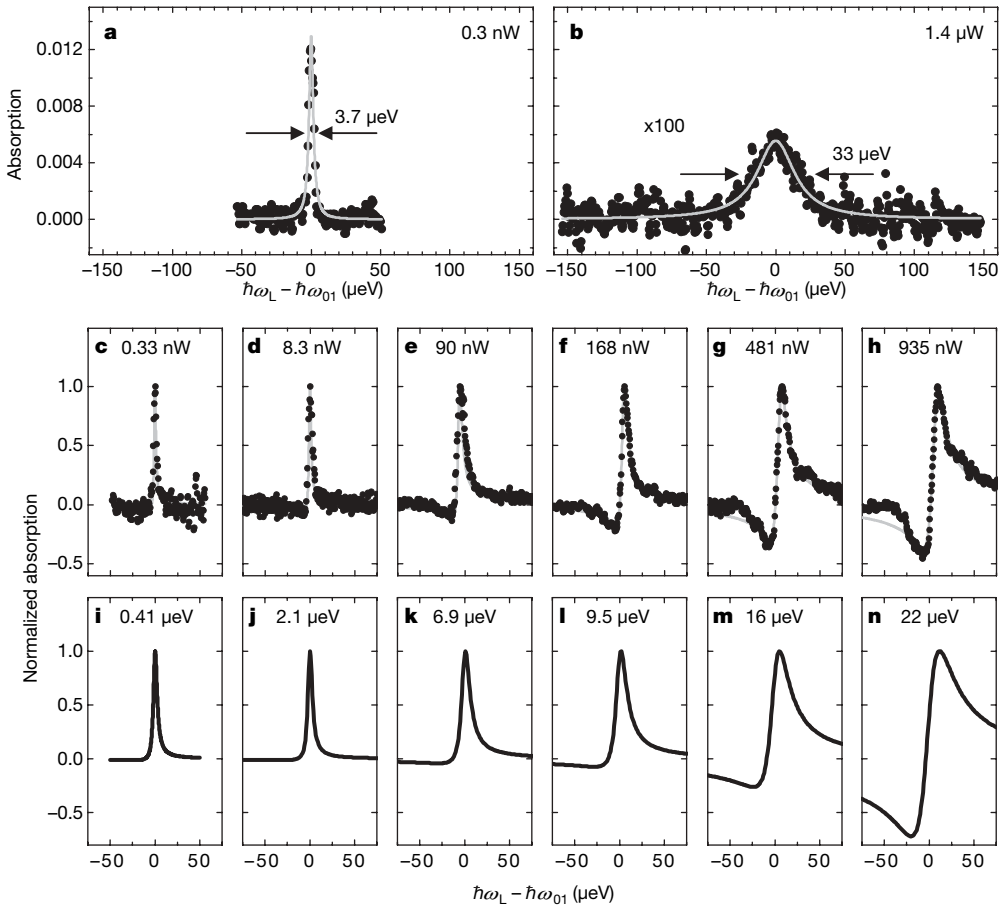

Figure 2 | Laser spectroscopy on a single quantum dot. a, **b**, Absorption of a single quantum dot from sample 1, exhibiting two-level behaviour, plotted against detuning for two laser intensities, 0.3 nW in the linear regime (**a**), and 1.4 μW in the nonlinear regime (**b**). The solid lines are lorentzian fits to the data. The observed nonlinear behaviour indicates that the dot has no significant coupling to extended electronic states of the crystal. **c**–**h**, X^{1-} absorption spectra from a single dot from sample 2 for several different laser powers as indicated in the figure; the absorption spectrum is given by the change in transmission $\Delta T(\delta)/T$, where $\delta = \omega_L - \omega_{01}$ is the detuning and T is the transmission. Symbols represent the experiment, solid lines are a guide to the eye based on Fano's theory. **i**–**n**, Absorption spectra as calculated with the theory described in the text with parameters: $\hbar\gamma_{10} = 2.16$ μeV, $q = 12$, $\Delta = 0.4$ μeV and $\hbar\gamma_{20} = 30$ μeV. The Rabi energies ($\hbar\Omega_{01}$) indicated in the panels correspond to the laser powers of the experiment. The data were measured at 4.2 K with a wavelength of ~950 nm on the X^{1-} resonance.

contact with the continuum: the combination of applied electric field and large capping thickness enables the hole to tunnel out of the dot into an empty continuum state[23], $|k\rangle$ (Fig. 1c). The final state of the transition is therefore hybridized with the continuum. Furthermore, a weak optical transition must also exist between $|0\rangle$ and $|k\rangle$. The two conditions for the Fano effect—two competing optical pathways and a hybridized excited state—are satisfied. The tunnelling involves a bound hole and the valence states at the capping layer–blocking barrier interface, which have a two-dimensional (2D) character. The tunnelling rate is non-zero when the localized hole level is within the 2D continuum of hole states in the quantum well[23]. This is the explanation for the bias dependence in Fig. 3b: at gate voltage $V_g > -0.22$ V, the quantum dot state moves out of the 2D continuum, the hybridization with the continuum vanishes and $1/q \rightarrow 0$. The modelling of $1/q(V_g)$ confirms our picture of tunnelling (Fig. 3b and Supplementary Materials). We stress that virtually any dot in sample 2 shows a nearly symmetric line at low power with quite large q ($\sim$12), and strongly asymmetric Fano lines at elevated powers.

We present a quantum mechanical model of these processes. Fano's original theory[1] applies for a weak driving field where hybridization arises between basis states $|1\rangle$ and $|k\rangle$. The classic case is the doubly excited state of the He atom. This state can auto-ionize (Fig. 1a). In the presence of a strong driving field, the mathematics is doubly difficult but nevertheless analytical results for atomic systems exist[9,24]. However, the solid-state systems are very different and require a new theory. First, in our case, the quantum dot ground state $|0\rangle$ is repopulated through tunnelling from the reservoir. In the atomic case, the Fano resonance leads to photoionization—excited electrons are ejected at high speed and never return. The large time limits are therefore different: in the quantum dot case, the steady state corresponds to non-zero absorption; in the atomic case it does not, as the system becomes ionized and absorption vanishes. Second, energy relaxation processes are crucial in the quantum dot system but not in the atomic system. For instance, the autoionization rate of the $2s^12p^1$ He atom state $|1\rangle \rightarrow |k\rangle$ is much faster than spontaneous emission and $q \approx 1$, whereas in our sample 2, the tunnelling rate, $\Delta/\hbar$, is less than the spontaneous emission rate, $\Delta/\hbar \leq \gamma_{10}$, and $q \gg 1$; here Δ and γ_{10} represent the tunnel broadening and spontaneous emission rate, respectively. In this sense, quantum dot quantum optics can be very different to atom optics as the parameters and conditions can be widely different and controllably designed.

We present a generalized theory for a closed system. The levels in our model are sketched in Fig. 1d: a ground state, $|0\rangle$, a single exciton state $|1\rangle$, and a set of continuum states, $|k\rangle$. Optical absorption processes are described by the matrix elements (Rabi frequencies) Ω_{01} and Ω_{0k}. States $|1\rangle$ and $|k\rangle$ are connected by a tunnel matrix element, γ_{tun}. Fast relaxation in the continuum states is described with a relaxation rate γ_{k2} from state $|k\rangle$ to a shelving state $|2\rangle$; repopulation from $|2\rangle$ to $|0\rangle$ is described by rate γ_{20}. In practice, hole tunnelling leaves behind two electrons in the dot. The hole relaxes rapidly on a picosecond timescale to the bottom of the 2D hole continuum; of the two electrons in the dot, one tunnels out to the back contact on a timescale of $\sim$10 ps (ref. 25) and it is this tunnelling process that is described with rate γ_{20}. The X^{1-} spectra are recorded in the voltage interval where the electron state is stable owing to the strong Coulomb blockade, allowing us to neglect Kondo-like processes[26]. In order to include the various relaxation processes, we perform the calculation with a master equation for the density matrix. We obtain an analytic result for the optical absorbed power, $Q(\delta)$ (where δ is the detuning of the laser from the resonance; see below), under the realistic assumption of a small population of the continuum states; indeed, filling of the states in the continuum would require very large powers. The resulting equation is rather complex (equation (S2), Supplementary Information) but yields the correct limit in the linear regime, $\Omega_{01} \ll \gamma_{10}$:

$$Q(\delta) = \hbar^2 \Omega_{01}^2 \frac{\omega_L}{2q^2\Delta}\left(1 + \frac{\gamma(q^2-1)(\Delta/\hbar)}{\gamma^2+\delta^2} + \frac{2q\delta(\Delta/\hbar)}{\gamma^2+\delta^2}\right) \quad (1)$$

where $\delta = \omega_L - \omega_{01}$, the detuning of the laser ($\hbar\omega_L$) from the resonance ($\hbar\omega_{01}$); $\Delta = \pi\hbar^2\gamma_{tun}{}^2\rho$, the tunnel broadening where ρ is the density of continuum states; $q = \hbar\gamma_{tun}\Omega_{01}/\Delta\Omega_{0k}$, the Fano factor; and $\gamma = \gamma_{10} + \Delta/\hbar$. We assume here that the effective width of the 2D continuum is much larger than Ω_{01} and Δ. This is similar to saying that γ_{tun} is a slowly varying function of k and gate voltage (see Supplementary Materials). The final term in equation (1) is negligible when $q >> 1$ and $\Delta/\hbar < \gamma_{10}$, leading to an almost symmetric lineshape. In other words, the tunnel coupling is masked by strong radiative damping. In the limit $\Omega_{01} >> \Delta/\hbar, \gamma_{10}$, the line becomes symmetric but instead of a maximum it has a minimum at $\delta = 0$:

$$Q(\delta) = \hbar^2 \Omega_{01}^2 \frac{\omega_L}{2q^2\Delta}\left(1 - \frac{(q^2+1)\Omega_{01}^2}{4q^2\delta^2 + 2(q^2+1)\Omega_{01}^2}\right) \quad (2)$$

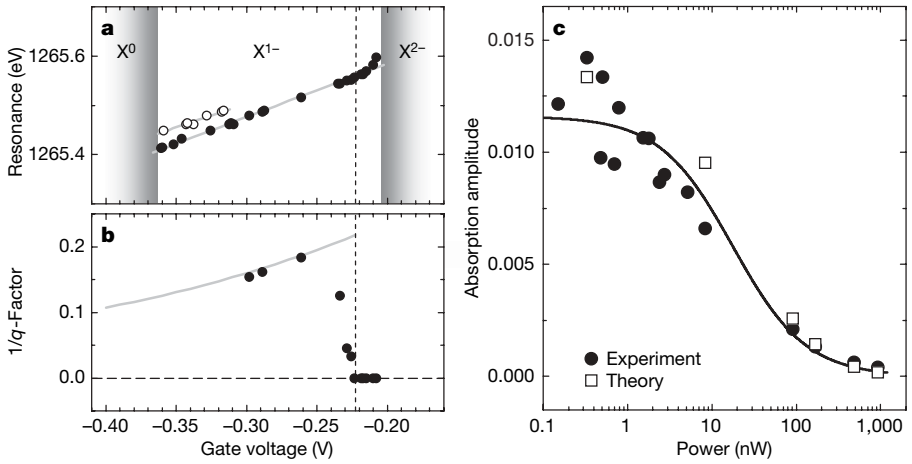

Figure 3 | Voltage dependence of the Fano resonance. a, Energy of the X^{1-} resonance ($\hbar\omega_{01}$) as a function of gate voltage (filled circles). The X^{1-} is observed in the window of gate voltages between -0.36 V and -0.205 V as a result of Coulomb blockade. At the low energy side of the plateau a second resonance line appears, as depicted by the open circles. The vertical dashed line shows the onset of the asymmetry, and the solid line represents the linear Stark effect. **b**, $1/q$ versus gate voltage at a constant power of 200 nW. At gate voltages below -0.3 V, the second peak hinders the fitting of the spectra. The solid line reflects the calculated voltage dependence of $1/q$ (see Supplementary Materials). The horizontal dashed line represents the zero level. **c**, The measured absorption amplitude of the resonance as a function of laser power is plotted, as well as the amplitudes predicted by the theory with the parameters in Fig. 2. The line represents a two-level model as a guide to the eye.

This behaviour corresponds to a 'negative resonance' or strongly destructive interference in the limit of very large power. At realistic, finite Ω_{01}, the destructive interference shows up as a large undershoot to the resonance with a zero crossing (Fig. 2n).

The experimental data in Fig. 2 are given for the absorption coefficient $\alpha = \Delta T/T = Q(\delta)/P$, where T and P are the transmission and light power, respectively. In the linear regime, the maximum absorption coefficient depends on the laser spot area A as $\alpha_0 = 3(\lambda/n)^2/(2\pi A)$, where λ and n are the laser wavelength and material refractive index, respectively. This expression for α_0 follows from ${\Omega_{01}}^2 = 2\alpha_0\gamma_{10}P/(\hbar\omega_L)$ (ref. 20). We compare the theory to the experimental data by taking the known values of γ_{10}, by determining q through a fit to the data at low power, and then adjusting Δ and γ_{20} to account for the data at high power. We find very good agreement with the theory (Fig. 2i–n and Fig. 3c). Here Δ is small because the tunnel coupling is weak. Simultaneously, q is large because the inter-band optical element Ω_{0k} is small.

The significance of the negative signals in Fig. 2 is that even very weak coupling to the continuum becomes easy to detect by enhancing the interference at large laser power. At small power, the fundamental spontaneous emission process destroys the interference effect. In principle, the spontaneous emission could be suppressed in a detuned microcavity[16,27]. However, this method is very challenging technologically, and would require elaborate sample preparations. Our method is certainly more flexible. In the control sample 1, it now becomes striking that there are no hints of the Fano effect even at the highest power, demonstrating that in this case, the quantum dot behaves very much like a few-level system. We should note that, with the nonlinear Fano effect, we are able to suppress the role of spontaneous emission dephasing in our quantum dots; however, other types of dephasing need to be analysed specially and, in principle, they may wash out the Fano asymmetry. Fortunately, the exciton resonance in our dots is predominantly dephased by spontaneous emission[10].

Two overriding points emerge. The first is the tunability of the quantum dot system: Fano effects can be turned on and off. The second is that the nonlinear Fano effect can be used to detect very weak interactions with continuum states in quantum systems. The nature of the interaction is not restricted: tunnelling, Auger processes and Foerster transfer are all included[28]. We note that a very strong nonlinear Fano effect was also observed on p-doped samples, in which the continuum of states is most probably generated by impurity states due to the doping atoms. The nonlinear Fano resonance described here could be produced by interactions of many different types—this is because the three-state scheme demonstrating the quantum interference effect (Fig. 1 c) is generic, and appears in a variety of physical systems, including solids, atoms, molecules and photonics.

Received 7 August; accepted 22 November 2007.

1. Fano, U. Effects of configuration interactions on intensities and phase shifts. *Phys. Rev.* **124,** 1866–1878 (1961).
2. Madden, R. P. & Codling, K. New autoionizing atomic energy levels in He, Ne, and Ar. *Phys. Rev. Lett.* **10,** 516–518 (1963).
3. Cerdeira, F., Fjeldly, T. A. & Cardona, M. Effect of free carriers on zone-center vibrational modes in heavily doped p-type Si. II. Optical modes. *Phys. Rev. B* **8,** 4734–4745 (1973).
4. Hase, M., Demsar, J. & Kitajima, M. Photoinduced Fano resonance of coherent phonons in zinc. *Phys. Rev. B* **74,** 212301 (2006).
5. Faist, J., Capasso, F., Sirtori, C., West, K. W. & Pfeiffer, L. N. Controlling the sign of quantum interference by tunnelling from quantum wells. *Nature* **390,** 589–592 (1997).
6. Schmidt, H., Campman, K. L., Gossard, A. C. & Imamoglu, A. Tunneling induced transparency: Fano interference in intersubband transitions. *Appl. Phys. Lett.* **70,** 3455–3457 (1997).
7. Bar-Ad, S., Kner, S., Marquezini, M. V., Mukamel, S. & Chemla, D. S. Quantum confined Fano interference. *Phys. Rev. Lett.* **78,** 1363–1366 (1997).
8. Wagner, J. & Cardona, M. Electronic Raman scattering in heavily doped p-type germanium. *Phys. Rev. B* **32,** 8071–8077 (1985).
9. Rzazewski, K. & Eberly, J. H. Confluence of bound-free coherences in laser-induced autoionization. *Phys. Rev. Lett.* **47,** 408–412 (1981).
10. Högele, A. *et al.* Voltage-controlled optics of a quantum dot. *Phys. Rev. Lett.* **93,** 217401 (2004).
11. Zrenner, A. *et al.* Coherent properties of a two-level system based on a quantum dot photodiode. *Nature* **418,** 612–614 (2002).
12. Gammon, D. & Steel, D. G. Optical studies of single quantum dots. *Phys. Today* **55,** 36–41 (2002).
13. Stufler, S., Ester, P., Zrenner, A. & Bichler, M. Quantum optical properties of a single $In_xGa_{1-x}As$-GaAs quantum dot two-level system. *Phys. Rev. B* **72,** 121301(R) (2005).
14. Reithmaier, J. P. *et al.* Strong coupling in a single quantum dot-semiconductor microcavity system. *Nature* **432,** 197–200 (2004).
15. Yoshie, T. *et al.* Vacuum Rabi splitting with a single quantum dot in a photonic crystal nanocavity. *Nature* **432,** 200–203 (2004).
16. Peter, E. *et al.* Exciton-photon strong-coupling regime for a single quantum dot embedded in a microcavity. *Phys. Rev. Lett.* **95,** 067401 (2005).
17. Hennessy, K. *et al.* Quantum nature of a strongly coupled single quantum dot-cavity system. *Nature* **445,** 896–899 (2007).
18. Warburton, R. J. *et al.* Optical emission from a charge-tunable quantum ring. *Nature* **405,** 926–929 (2000).
19. Loudon, R. *The Quantum Theory of Light* 3rd edn (Oxford Univ. Press, Oxford, 2000).
20. Kroner, M. *et al.* Resonant saturation laser spectroscopy of a single self-assembled quantum dot. *Physica E* (in the press).
21. Alén, B. *et al.* Absorptive and dispersive optical responses of excitons in a single quantum dot. *Appl. Phys. Lett.* **89,** 123124 (2006).
22. Atatüre, M. *et al.* Observation of Faraday rotation from a single confined spin. *Nature Phys.* **3,** 101–105 (2007).
23. Seidl, S. *et al.* Absorption and photoluminescence spectroscopy on a single self-assembled charge tunable quantum dot. *Phys. Rev. B* **72,** 195339 (2005).
24. Rzazewski, K. & Eberly, J. H. Photoexcitation of an autoionizing resonance in the presence of offdiagonal relaxation. *Phys. Rev. A* **27,** 2026–2042 (1983).
25. Smith, J. M. *et al.* Voltage control of the spin dynamics of an exciton in a semiconductor quantum dot. *Phys. Rev. Lett.* **94,** 197402 (2005).
26. Govorov, A. O., Warburton, R. J. & Karrai, K. Kondo excitons in self-assembled quantum dots. *Phys. Rev. B* **67,** 241307(R) (2003).
27. Bayer, M. *et al.* Inhibition and enhancement of the spontaneous emission of quantum dots in structured microresonators. *Phys. Rev. Lett.* **86,** 3168–3171 (2001).
28. Zhang, W., Govorov, A. O. & Bryant, G. W. Semiconductor-metal nanoparticle molecules: hybrid excitons and non-linear Fano effect. *Phys. Rev. Lett.* **97,** 146804 (2006).

Supplementary Information is linked to the online version of the paper at www.nature.com/nature.

Acknowledgements We thank A. Högele for discussions and J. P. Kotthaus for support. The work was supported by SFB 631 (Germany), AvHF (Germany), EPSRC (UK), NSF (USA) and SANDiE (EU). B.D.G. thanks the Royal Society of Edinburgh for financial support. Financial support from the German Excellence Initiative via the Nanosystems Initiative Munich (NIM), and from Ohio University Nanobiotechnology Initiative, is acknowledged.

Author Information Reprints and permissions information is available at www.nature.com/reprints. Correspondence and requests for materials should be addressed to A.O.G. (govorov@helios.phy.ohiou.edu).